

# Observation of Nonlinear Mode in a Cylindrical Fabry-Perot Cavity

Jack Boyce, Juan P. Torres and Raymond Y. Chiao

*Department of Physics, University of California, Berkeley, California 94720*

*Voice: (510) 642-5620 Fax: (510) 643-8497*

## Abstract

We report the first observation of a nonlinear mode in a cylindrical nonlinear Fabry-Perot cavity. The field enhancement from cavity buildup, as well as the large  $\chi^{(3)}$  optical nonlinearity due to resonantly-excited  $^{85}\text{Rb}$  vapor, allows the nonlinear mode to form at low incident optical powers of less than a milliwatt. The mode is observed to occur for both the self-focusing and self-defocusing nonlinearity.

Self-trapping and self-focusing effects due to the nonlinear response of materials to an applied optical field have been an interesting topic of research from the early days of nonlinear optics [1]. Most work has been done in traveling-wave systems, where waveguides and pulsed lasers are used to achieve large intensities and enhanced nonlinear effects. Spatial solitons have become a widespread paradigm in explaining many nonlinear effects [2], and have been observed in Kerr [3,4],  $\chi^{(2)}$  [5,6], and photorefractive [7] media. In a cavity geometry, the main concern has been to explore optical bistability for its potential applications such as all-optical switching [8].

In a linear cavity there are specific beam profiles that result in transmissivity, defined as the ratio of the transmitted power to the incident power, being equal to unity. These are the so-called longitudinal and transverse modes of the cavity. In a cavity with planar mirrors these modes are plane waves; such a cavity driven by a finite-sized beam yields a transmissivity less than unity due to diffraction. Notwithstanding, peaks in the transmissivity exist for frequencies corresponding to the longitudinal modes. When the cavity is filled with a nonlinear medium, other peaks in the transmissivity occur when the nonlinearity induces a resonance. We will refer to them as *nonlinear modes*, i.e., nonlinear spatial patterns whose fields oscillate everywhere at the same frequency inside the cavity. In this Letter we report the observation of a nonlinear mode in a cylindrical Fabry-Perot cavity [9] filled with atomic rubidium vapor. The cavity-field buildup and resonantly-enhanced nonlinearity give stronger nonlinear effects for a given incident beam intensity than do the traveling-wave configurations, permitting our use of a low-power CW diode laser.

To study 1D transverse nonlinear optical effects, the experiment consists of a cylindrical Fabry-Perot cavity illuminated with an incident beam  $E_{inc}$ , as shown in Fig. 1, and filled with a material having a Kerr nonlinearity ( $n = n_0 + n_2|E|^2$ ). The mirror curvature in the  $y$ -dimension causes strong single-moding in that direction, and a single longitudinal mode is excited. The most important dynamics are in the  $x$ -dimension, where the field is determined by the combined effects of self-(de)focusing and diffraction. The field envelope within the cavity, in the mean field limit, evolves according to a damped, driven version of the nonlinear

Schrödinger equation [10,11]

$$\frac{\partial E}{\partial t} = \frac{ic}{2n_0k} \frac{\partial^2 E}{\partial x^2} + i\omega A \frac{n_2}{n_0} |E|^2 E + \frac{ic\Delta k}{n_0} E - \Gamma(E - E_d), \quad (1)$$

where  $E(x, t)$  is the internal cavity field envelope amplitude,  $k$  is the longitudinal wavenumber,  $\omega = ck/n_0$  is the field angular frequency,  $A = 3/4\sqrt{2}$  is a mode-overlap factor,  $\Delta k = k - k_L$  is the wavenumber mismatch within the cavity of a weak driving field from linear-response plane-wave resonance,  $\Gamma = c(\mathcal{T} + \alpha L)/2n_0L$  is the amplitude decay rate ( $\mathcal{T}$  is the intensity transmission coefficient at each mirror, assumed equal,  $L$  is the cavity length,  $\alpha$  is the absorption coefficient due to the intracavity material, and  $\mathcal{T} + \alpha L \ll 1$ ), and  $E_d(x)$  is the driving field, which is proportional to the incident field. In our experiment each of the terms on the right of Eq. 1 is comparable in magnitude.

The experimental arrangement used to observe the spatial nonlinear mode in a Fabry-Perot cavity is shown in Fig. 2. A 35 mW, 780 nm Sharp diode laser with external grating feedback (PZT-tuned) is used as the light source. After a variable attenuator and a spatial filter, the beam travels through a 3-element cylindrical telescope used to control the beam waist in the  $x$ -direction to between 30 and 300  $\mu\text{m}$  at the cavity input face. A cylindrical mode-matching lens focuses in the  $y$ -direction to efficiently couple into the cavity's lowest-order transverse mode. The CCD camera and photodiode D3 image the light leaving the exit mirror of the cavity. Two additional detectors are also used in the experiment: detector D1 is used primarily for alignment (it only receives appreciable power when the beam is collimated in  $x$  and mode-matched in  $y$ , at the cavity input face), and detector D2 monitors input power.

The nonlinear Fabry-Perot cavity itself consists of two mirrors, one cylindrical and the other planar, separated by  $L = 4.5$  mm and with  $\mathcal{T} \approx 0.007$ . The cavity length and alignment are precisely tunable using 3 micrometers and piezoelectric elements on the planar mirror. The concave mirror has a cylindrical radius of curvature of 9.8 mm, yielding a mode beam waist (1/e half-width in field profile) of 35  $\mu\text{m}$  in the  $y$ -direction. The cavity is filled with natural-abundance rubidium vapor at an atomic number density of  $N = 1.5 \times 10^{12} \text{ cm}^{-3}$ .

The laser light excites the atoms on their D2 transition near 780 nm to provide a resonantly-enhanced optical nonlinearity. Figure 3 shows the calculated linear absorption and nonlinear index  $n_2$ , including Doppler broadening and all hyperfine magnetic sublevels. The arrow in Fig. 3 indicates the line used in the experiment, corresponding to transitions out of the  $^{85}\text{Rb}$ ,  $F = 2$  ground-state hyperfine level. This line was chosen due to its relative strength and separation in frequency from other lines.

Figure 4 shows an example of the variation in optical power transmitted through the cavity as the laser frequency is scanned at a rate of 20 Hz, for 0.82 mW of incident power (beam waists of  $130\ \mu\text{m}$  and  $35\ \mu\text{m}$  in the  $x$  and  $y$  dimensions, respectively) and a fixed cavity length  $L$ . Bistability (a dependence on scanning direction) is not observed. The transmission peak marked “linear” corresponds to the ordinary linear Fabry-Perot transmission resonance. The asymmetry of this resonance is primarily due to the linear index and absorption of the atomic vapor. The “nonlinear” peak is observed to be power-dependent in two ways: firstly, it shifts in frequency as a function of the incident laser intensity, and secondly, it disappears at sufficiently low intensity. This peak occurs where the nonlinear index change is sufficient to shift the red-detuned laser into cavity resonance. As incident beam power is decreased, it moves toward atomic line center, away from the linear resonance. Once a maximum frequency shift is reached, the nonlinear resonance peak smoothly vanishes as the incident power is further decreased. This peak is thus the nonlinear mode. By contrast, the linear mode is observed not to change at all with power. The “Lamb” feature is due to the forward- and backward-going cavity beams saturating the atomic absorption at line center.

Transmission spectra for two different values of the cavity length  $L$  are compared in Fig. 5, using the same incident beam power and dimensions as above. There is a transmission enhancement in the nonlinear resonance on the blue side of the atomic line; this is due to the presence of self-focusing in the  $x$ -direction on that side, and self-defocusing on the other. In the former case the effect acts against diffraction to give more complete constructive interference in the forward direction, whereas in the latter case the nonlinearity acts *with* diffraction and the transmission is lower. Absorption complicates the spatial aspects of

nonlinear mode formation, but a comparison between the red- and blue-detuned cases in Fig. 5 is meaningful since absorption is symmetrical about line center.

Spatial profiles of the transmitted beams for two cases with equal atomic absorptions and opposite signs of  $n_2$  are shown in Fig. 6, again using 0.82 mW of incident power and Gaussian beam waists of  $130\ \mu\text{m}$  and  $35\ \mu\text{m}$  in the  $x$  and  $y$  dimensions, respectively. As discussed above the transmission is substantially higher when  $n_2 > 0$  and the width is also narrower in this case. The wavenumber mismatch  $\Delta k$  is measured using  $c\Delta k = n_0(\omega_{NL})\omega_{NL} - n_0(\omega_L)\omega_L$ , where  $\omega_{NL}$  and  $\omega_L$  are the measured frequencies of the nonlinear and linear resonances, respectively. We infer  $n_0(\omega)$  by measuring the frequency splitting of a linear cavity mode tuned exactly on atomic resonance (in our case the mode divides into two components at detunings of roughly  $\pm 500$  MHz relative to line center), and extrapolating to other frequencies using the known functional form of  $n_0(\omega)$  in a Doppler-broadened atomic vapor. The measured nonlinear mode widths  $\sigma$  (defined as the root-mean-square widths of the  $y$ -integrated intensity profiles) for the range  $10\ \text{m}^{-1} < |\Delta k| < 20\ \text{m}^{-1}$  are  $34.7\ \mu\text{m} < \sigma < 39.2\ \mu\text{m}$  for  $n_2 > 0$  and  $41.7\ \mu\text{m} < \sigma < 44.9\ \mu\text{m}$  for  $n_2 < 0$ , with the smaller widths corresponding to larger values of  $|\Delta k|$ .

In conclusion, we have demonstrated a new type of spatial nonlinear mode within a cylindrical nonlinear Fabry-Perot resonator. In the self-focusing case, some features of this mode are similar to spatial solitons in traveling-wave systems – numerical work indicates that the nonlinear mode has structural stability in the sense that the transmitted beam profile is insensitive to modest changes in the incident beam profile. The relationship between the cavity nonlinear mode and spatial solitons would be an interesting topic for further research.

This work was done with the support of the Office of Naval Research under ONR Grant Number N00014-99-1-0096, and of the National Science Foundation under NSF Grant Number 9722535. J.P. Torres is grateful to the Spanish Government for its support funded through the Secretaría de Estado de Universidades, Investigación y Desarrollo. We would also like to thank J. Bowie, J. Garrison, J. McGuire, and M. W. Mitchell for very helpful discussions.

## REFERENCES

- [1] R.Y. Chiao, E. Garmire, and C.H. Townes, Phys. Rev. Lett. **13**, 479 (1964); P.L. Kelley, Phys. Rev. Lett. **15**, 1005 (1965).
- [2] N.N. Akhmediev and A. Ankiewicz, *Solitons: Nonlinear Beams and Pulses*, Chapman-Hall, (1997).
- [3] A. Barthelemy, S. Maneuf, and C. Froehly, Opt. Commun. **55**, 201 (1985).
- [4] J.S. Aitchison, A.M. Weiner, Y. Silberberg, M.K. Oliver, J.L. Jackel, D.E. Leaird, E.M. Vogel, and P.W.E. Smith, Opt. Lett. **15**, 471 (1990).
- [5] R. Schiek, Y. Baek and G.I. Stegeman, Phys. Rev E, **53**, 1138 (1996).
- [6] W.E. Torruellas, Z. Wang, D.J. Hagan, E.W. Stryland, G.I. Torner, G.I. Stegeman and C.R. Menyuk, Phys. Rev. Lett. **74**, 5036 (1995).
- [7] G.C. Duree, Jr., J.L. Schultz, G.J. Salamo, M. Segev, A. Yariv, B. Crosignani, P. Di Porto, E.J. Sharp, R.R. Neurgaonkar, Phys. Rev. Lett. **71**, 533 (1993).
- [8] H.M. Gibbs, *Optical Bistability: Controlling Light with Light* (Academic Press, Orlando, 1985).
- [9] I.H. Deutsch, R.Y. Chiao, and J.C. Garrison, Phys. Rev. Lett. **69**, 3627 (1992).
- [10] L.A. Lugiato and R. Lefever, Phys. Rev. Lett. **58**, 2209 (1987).
- [11] J. Boyce and R.Y. Chiao, Phys. Rev. A **59**, 3953 (1999).

FIGURES

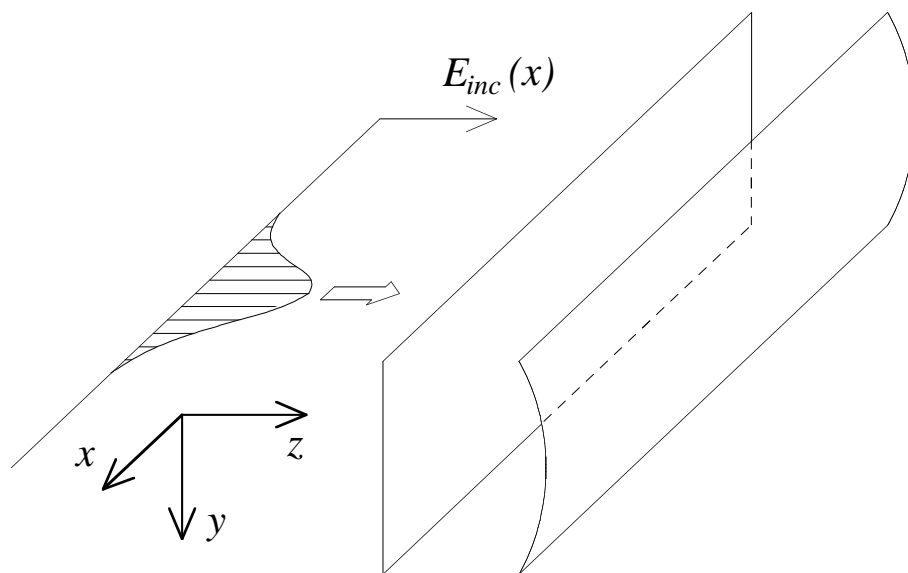


FIG. 1.

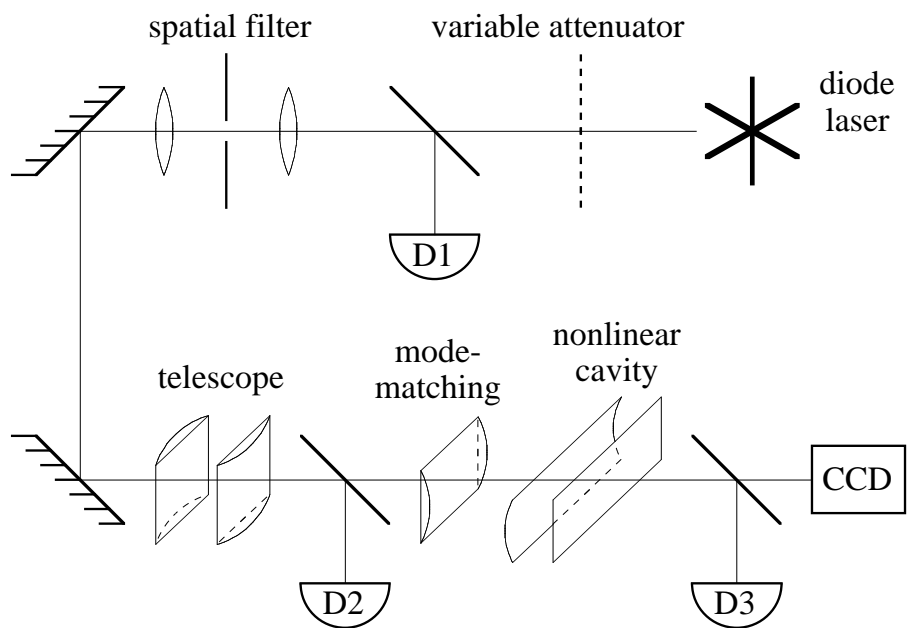


FIG. 2.

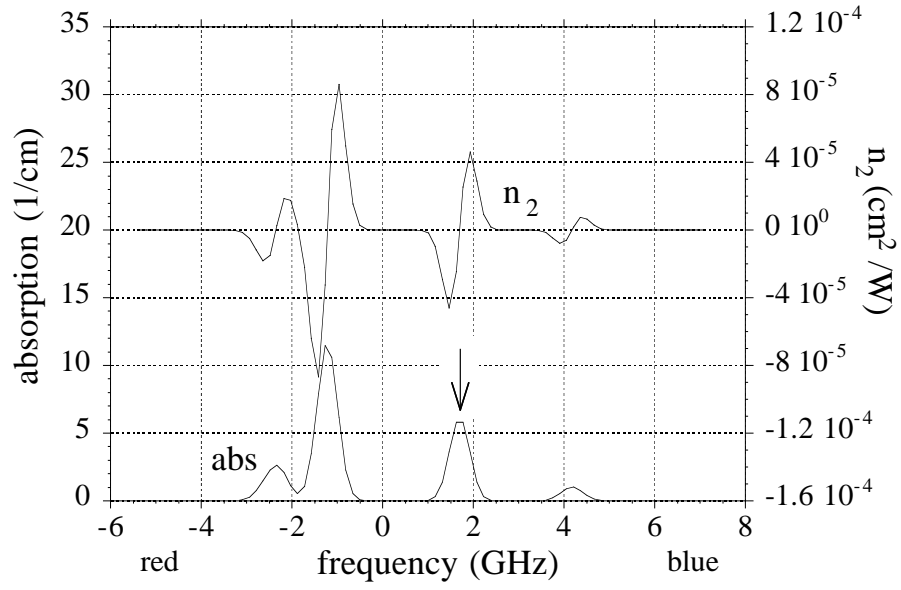


FIG. 3.

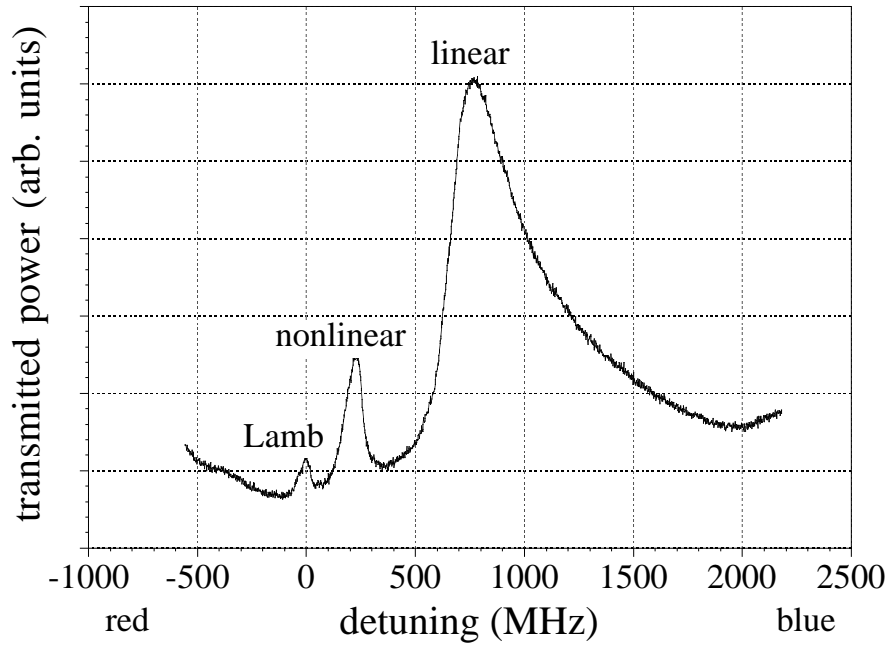


FIG. 4.

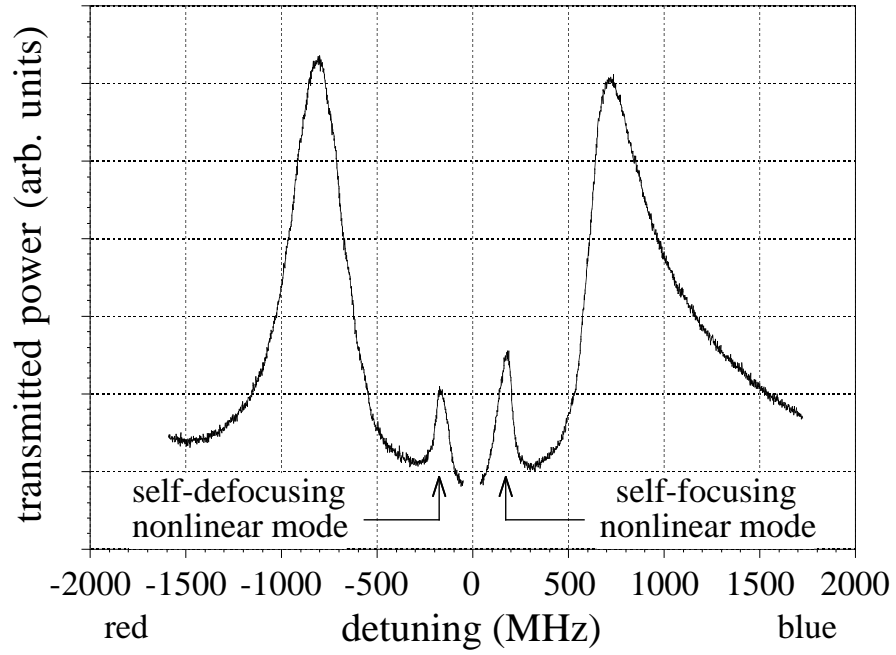


FIG. 5.

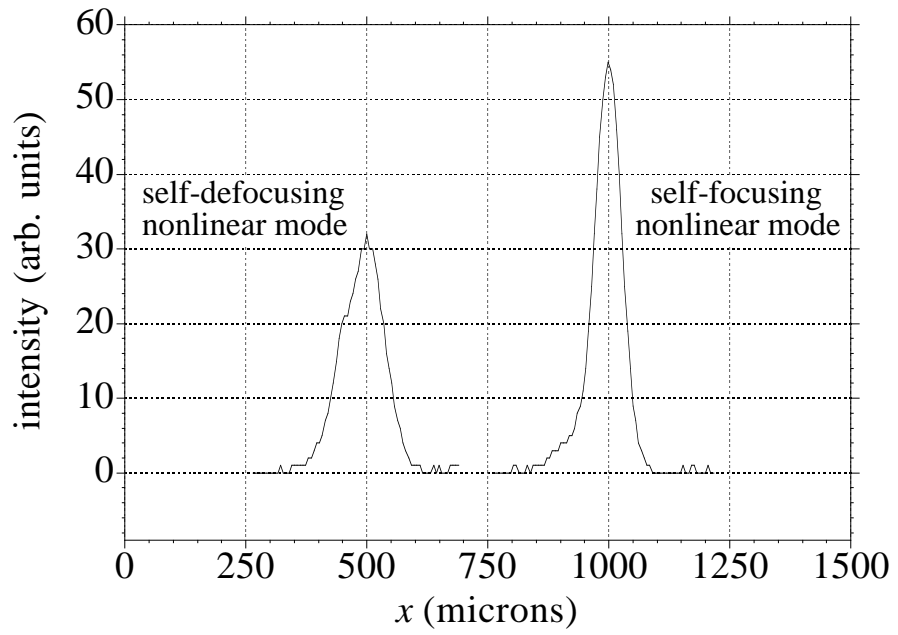


FIG. 6.

## FIGURE CAPTIONS

FIG 1. The cylindrical Fabry-Perot cavity, showing the coordinate system used and an incident Gaussian (in  $x$ ) beam.

FIG 2. Schematic of the experimental apparatus used to observe the spatial nonlinear mode. The D's are detectors.

FIG 3. Calculated linear absorption and  $n_2$  in natural-abundance Rb vapor at 80°C ( $N = 1.5 \times 10^{12} \text{ cm}^{-3}$ ), near the D2 transition at  $\lambda = 780 \text{ nm}$ , for circularly-polarized light. The arrow indicates the line used in the experiment, the Doppler-broadened  $^{85}\text{Rb}$ ,  $F = 2$  set of transitions.

FIG 4. Power transmitted through the nonlinear cavity as a function of laser frequency, for a particular cavity length  $L$  and beam power. Frequency is relative to the  $^{85}\text{Rb}$  line indicated in Fig. 3.

FIG 5. Total power transmitted through the cavity as a function of laser frequency, for two different cavity lengths  $L$ .

FIG 6. Transmitted intensity profiles of spatial nonlinear mode taken with the CCD camera, integrated over  $y$ , at the peaks of the nonlinear modes shown in Fig. 5.